

Chapter IV

Results

4.1 Appearance of Treated Rice Husk and Its Ash

After treatment, rice husk was changed due to the action of chemicals. The apparent change of rice husk after each step can give some clues on the effect of the respective treatment.

Tab. 6. Appearance of husk grains after different treatment

treatment	color	sensation on touching
None	very light brown	slightly brittle
NaOH	light brown	soft and flexible
HCl	dark brown	brittle
NaOH/HCl	dark grey-brown	extremely brittle
H ₂ SO ₄	brownish black	brittle
HNO ₃	saturated yellow	slightly brittle
Enzyme	very light brown	slightly brittle
Enzyme/HCl	brown	brittle
Enzyme/H ₂ SO ₄	dark brown	brittle

Tab. 7. Appearance of ash of treated husk

ash from treated husk	color & quality of incineration	sensation on touching
None	pink with some orange- brown grain and grey, black grain	stiff and brittle
NaOH	grey-black grain	very fine soft
HCl	white grain with very few black grain	crisp and brittle
NaOH/HCl	white fragmentary with some black husk grain pieces	very fine soft
H ₂ SO ₄	white grain with very few black grain	crisp and brittle
HNO ₃	white grain with some black-grey grain	crisp and brittle
Enzyme	homogeneous pink grain with very few grey part	crisp and brittle
Enzyme/HCl	white grain with very few black grain	crisp and brittle
Enzyme/H ₂ SO ₄	white grain with very few black grain	crisp and brittle

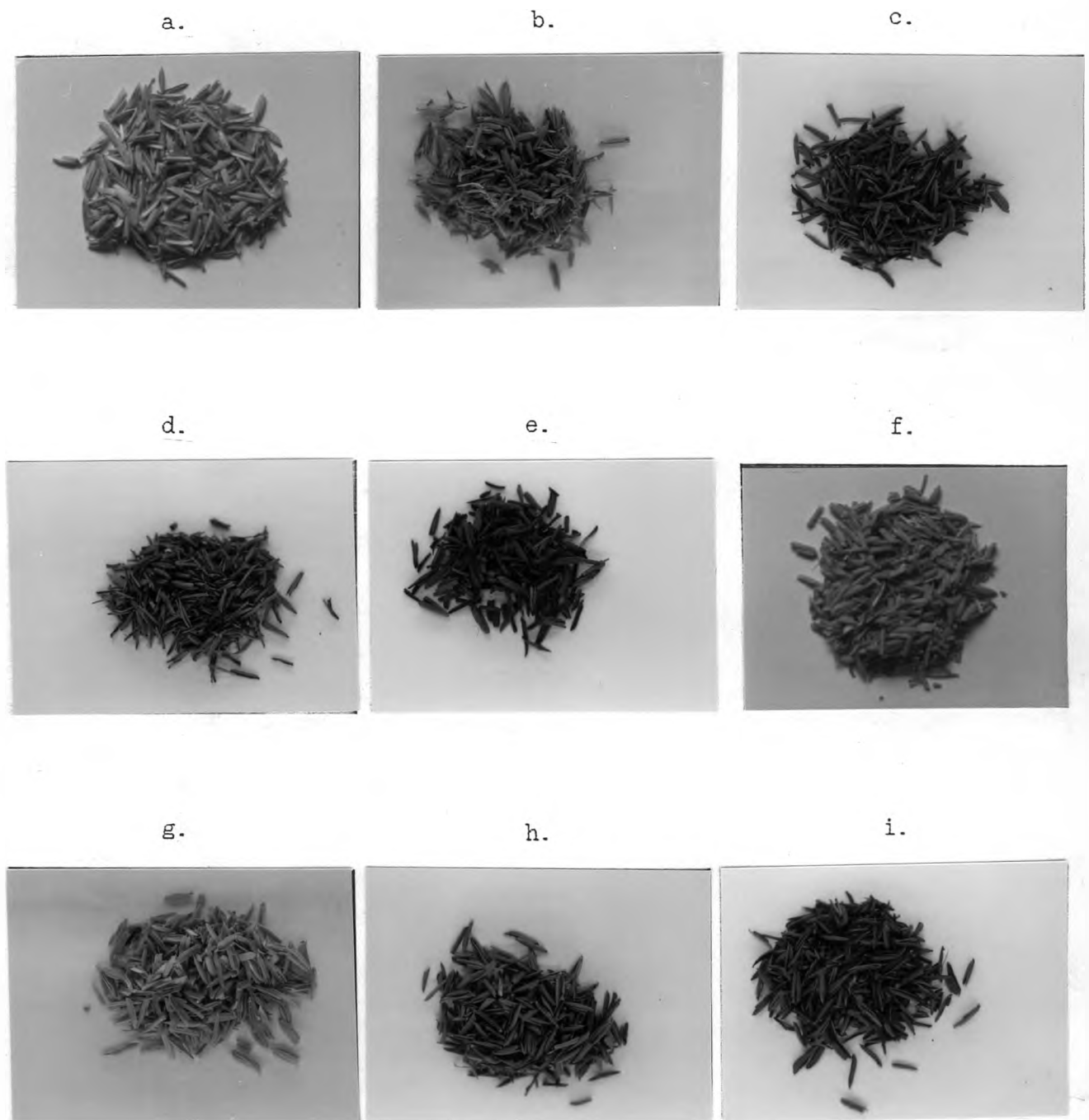


Fig. 14. Color impression of rice husk after different treatment
(a) No treatment; (b) NaOH treatment; (c) HCl treatment;
(d) NaOH/HCl treatment; (e) H_2SO_4 treatment; (f) HNO_3
treatment; (g) Enzymatic treatment; (h) Enzymatic/HCl
treatment; (i) Enzymatic/ H_2SO_4 treatment

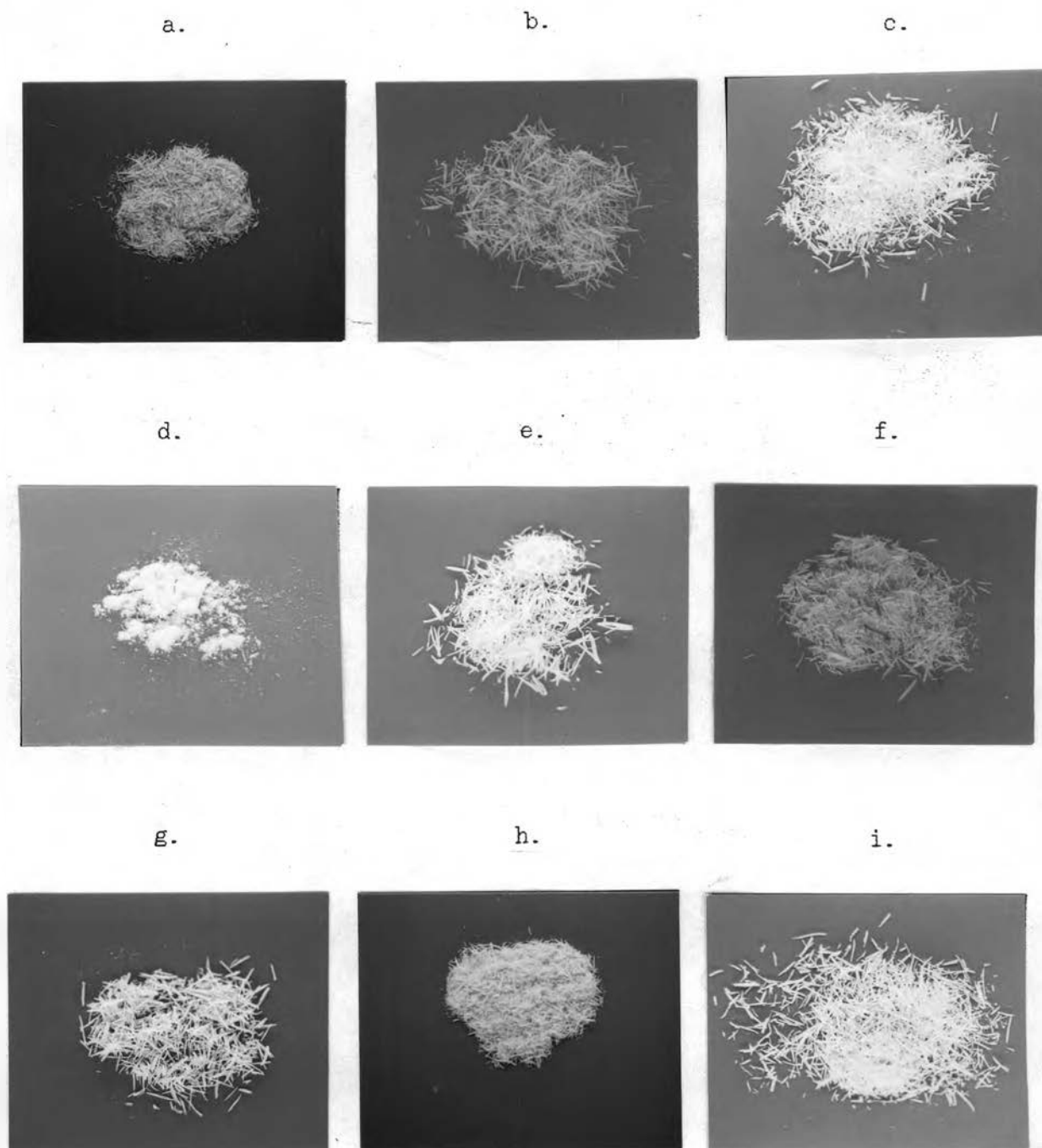


Fig. 15. Appearance of differently treated rice husk ash

(a) No treatment; (b) NaOH treatment; (c) HCl treatment;
(d) NaOH/HCl treatment; (e) H_2SO_4 treatment; (f) HNO_3
treatment; (g) Enzymatic treatment; (h) Enzymatic/HCl
treatment; (i) Enzymatic/ H_2SO_4 treatment

4.2 Weight Loss Determination

Tab. 8. Weight loss of rice husk treatment

treatment	loss in g during treatment of 100 g washed husk	loss in g on incineration of 100 g treated husk
None	-	77.1
NaOH	30.5	91.0
HCl	31.3	70.6
NaOH/HCl	53.0	91.7
H ₂ SO ₄	32.9	70.2
HNO ₃	32.9	77.0
Enzyme	7.5	76.6
Enzyme/HCl	29.5	69.4
Enzyme/H ₂ SO ₄	29.0	69.6

The leachants of each treatment had their specific smell and color. For HCl and H₂SO₄ treatment, the leachants smelled like wood oil, had a dark color and a lot of brown organic matter precipitated. But on HNO₃ treatment, the smell was weaker, and the color was bright yellow with few of yellow organic matter precipitated. With NaOH treatment, the leachant smelled badly, had an orange color and no precipitates. From enzymatic treatment, only a little bit turbid solution was received with a very weak smell.

From weight loss determination, the amount of ash samples after treatment and incineration were assessed.

Tab. 9. Rest from treatment and incineration

treatment	rest from initial ^{*)} 100 g after treatment of husk	rest from initial 100g after treatment and incineration
None	100.0	21 ^{**)}
NaOH	69.5	6.4
HCl	68.7	20.2
NaOH/HCl	47.0	3.9
H ₂ SO ₄	67.1	20
HNO ₃	67.1	15.4
Enzyme	92.5	21.6
Enzyme/HCl	70.5	21.6
Enzyme/H ₂ SO ₄	71.0	21.6

^{*)} washed husk; loss upon washing was 8.5 %

^{**)} may fluctuate by ± 1 (estimated)

As said before, chemical and enzymatic treatment were used to extract ash at high yield with low amount of impurities and with preserved nanostructure. Untreated husk gives the total amount of silica (including impurities). So we may conclude that the max. yield of ash is approx. 21 g/100 g. The color of ash can tell qualitatively

how much of organic residues are left. Chemical and enzymatic treatment did not only extract organic matter but also some inorganic matter (impurities, and silica). This can be known from ash weight of treated husk after incineration. NaOH and NaOH/HCl treatment was not suitable for the purpose, because NaOH reacts with silica and extracts major amounts of silica. HNO₃ treatment is better, but yields high loss of ash. By contrast, the remaining kinds of treatment, i.e., with HCl, H₂SO₄, enzyme, and combinations gave acceptable ash yields.

4.3 Crystallinity

All samples showed the typical amorphous hump around 22°, however, no indication of the formation of cristobalite or any other crystalline phase. By contrast, pre-treatment with NaOH resulted in a distinct peak at 29.5°. The peak cannot be identified without doubts, it may represent a sodium silicate phase. This goes together with the chemical analysis reported in 4.6 showing that the ash contains 68 % of silica only. Treatment with HCl after the NaOH treatment yield an amorphous material again. A NaOH pretreated sample incinerated at 850°C, showed, beside minor peaks, the characteristic cristobalite peak at 21.9°. The received X-ray diffraction patterns are summarized in figure 16 , next page.

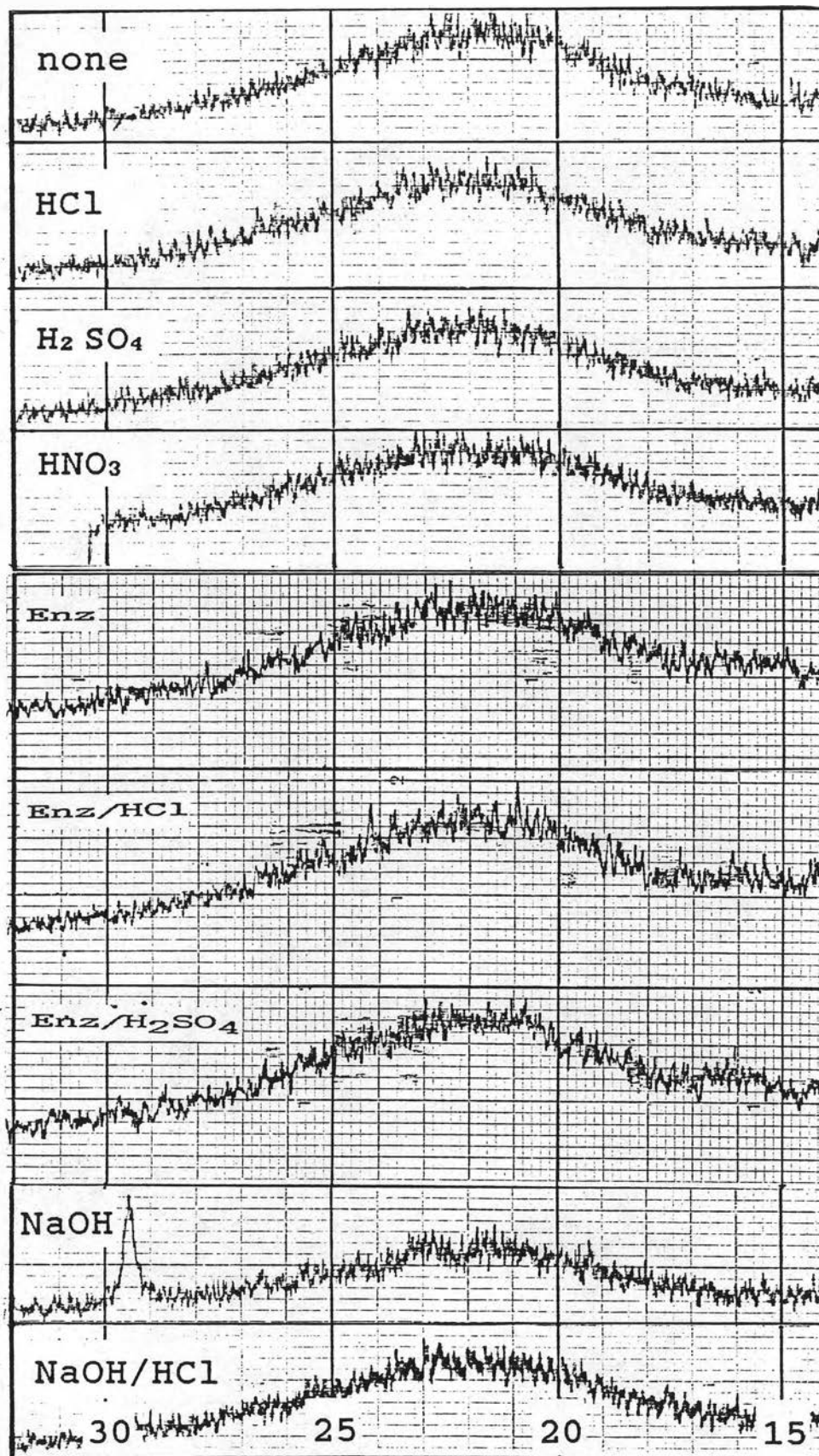


Fig. 16. X-ray diffraction patterns of rice husk ash prepared from differently pretreated husk ash

4.4 Morphology

4.4.1 Morphology of husk grains before, after treatment, and incineration by optical microscope and SEM.

Observation by optical microscope showed that the rice husk surface looked like a composite material, white grains dispersed on the yellow organic matrix. The white grains appear more clearly on the brown surface of treated husk. This may lead to the misunderstanding that the silica is majorly present as big white grains deposited on the organic matrix. But incinerated husk still displayed the same contours as before incineration. It only turned to be translucent.

The SEM micrograph series in figure 17 reveals a surprising view. The untreated husk (row 17 a-c), the charred husk (row 17 d-f), and the completely incinerated husk (row 17 g-i) virtually have the same appearance. If we consider that g-i contains > 99 % silica, then only one conclusion is possible: The entire epidermis of all samples consists of silica.

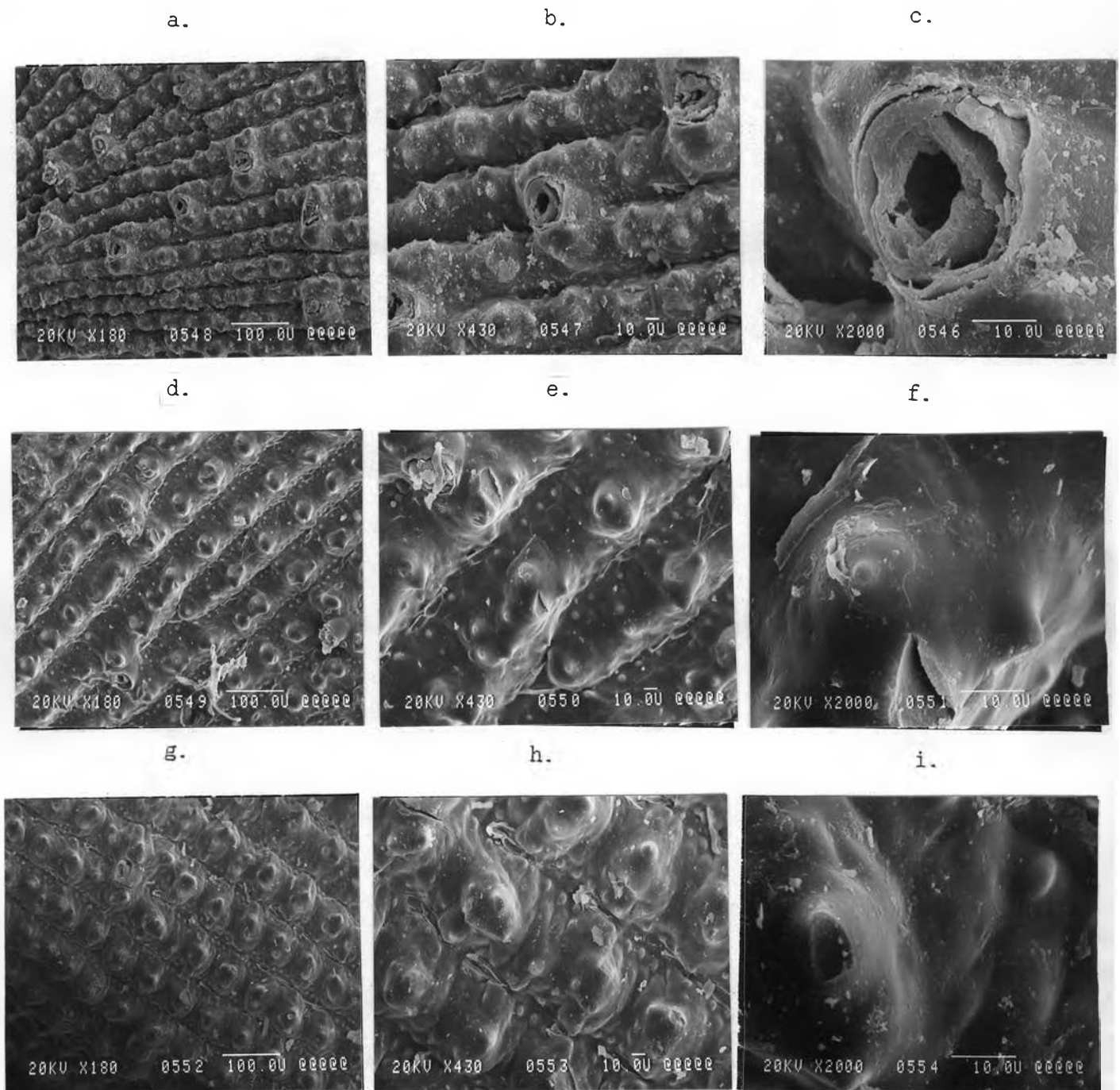





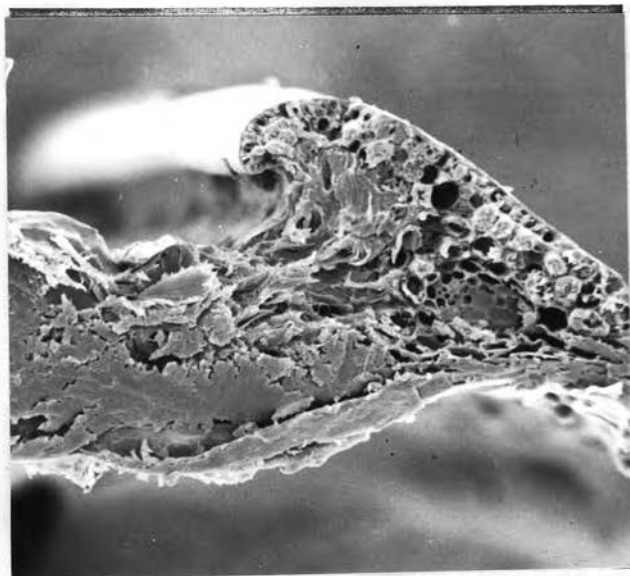
Fig. 17. SEM micrographs of uncombusted (a-c), pre-charred (d-f), and completely incinerated (g-i) rice husk grains;

a, d, g:  200 μm
 b, e, h:  50 μm
 c, f, i:  10 μm

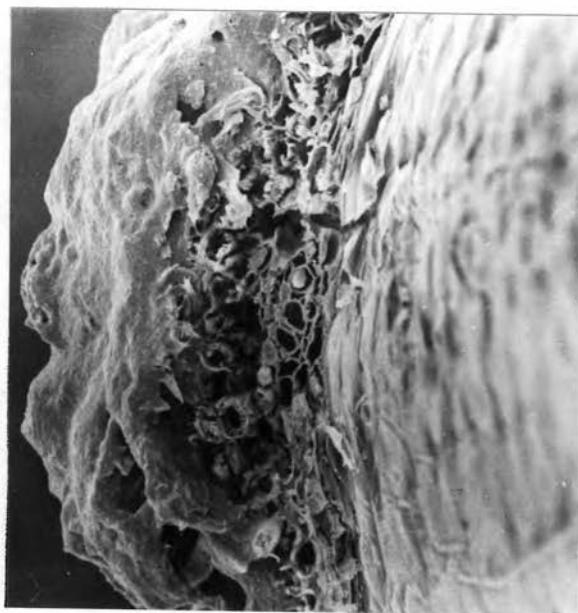
A more direct proof of this finding is tried by investigating cross sections. Results are shown in figure 18 a-c. These micrographs also give a clue to what happens with the organic matter during treatment. Again, the epidermis is not altered at all. Unfortunately, our SEM did not allow a mapping of Si at that time. However, we may consult a similar result by Nakata et al., 1989, figure 19. The series in figure 17, 18, and 19 provided a solid proof that the entire epidermis indeed consists of silica.

The SEM micrographs in figure 18 a. showed the parts of plant tissue in the inner part of non-treated rice husk. The xylem and phloem vessels are clearly visible. After the "soft" action of enzyme, figure 18 b., the plant tissue was still there. It can be concluded that the enzyme only shortened the polysaccharide chains (see 2.4) in situ without dissolving the glucose product. This resulted in low weight loss on enzymatic treatment. Acid treatment visibly extracted organic matter from the inner of rice husk. The findings are compatible with those of Nakata et al. (1989) and also Sharma et al. (1984) showing by different means that silica is deposited densely on the outer and inner epidermis of the individual grains.

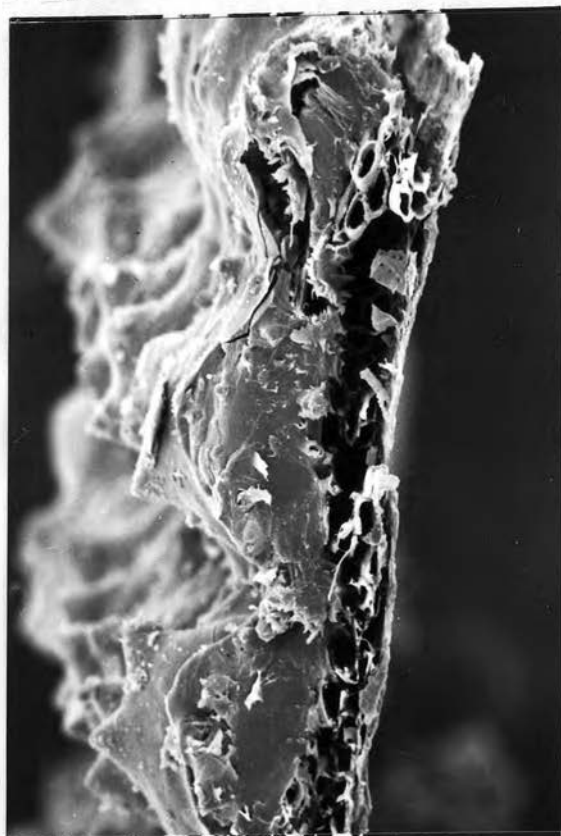
18 a.



18 b.



18 c.



19

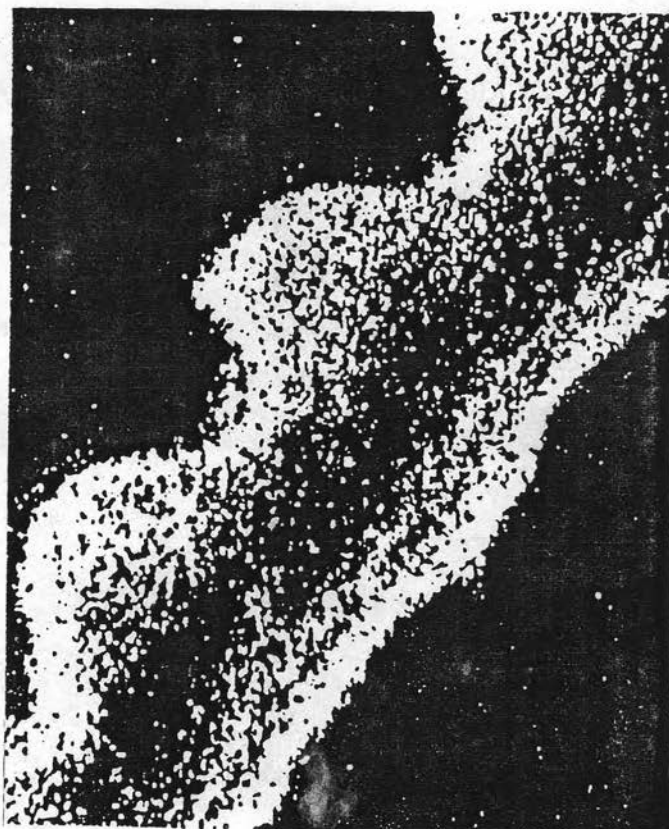


Fig. 18. Cross-section of a rice husk grain from a) No treatment, b) Enzymatic treatment, and c) Acid treatment |—| 20 μm

Fig. 19. X-ray mapping (Si) of a similar sample (Nakata et al., 1989)

|—| 20 μm

4.4.2 Morphology of husk ash powder by TEM and SEM

Rice husk ash powder was dispersed and particles of husk ash were shown in detail in TEM and SEM micrographs.

From TEM micrographs, next page, rice husk ash particles showed both globular and fractal agglomerates, by its own nature. But NaOH treated husk ash showed Ostwald ripening type neck growth as the treatment of this kind of husk occurred in solution at $\text{pH} > 10$, i.e., in the range of high silica solubility.

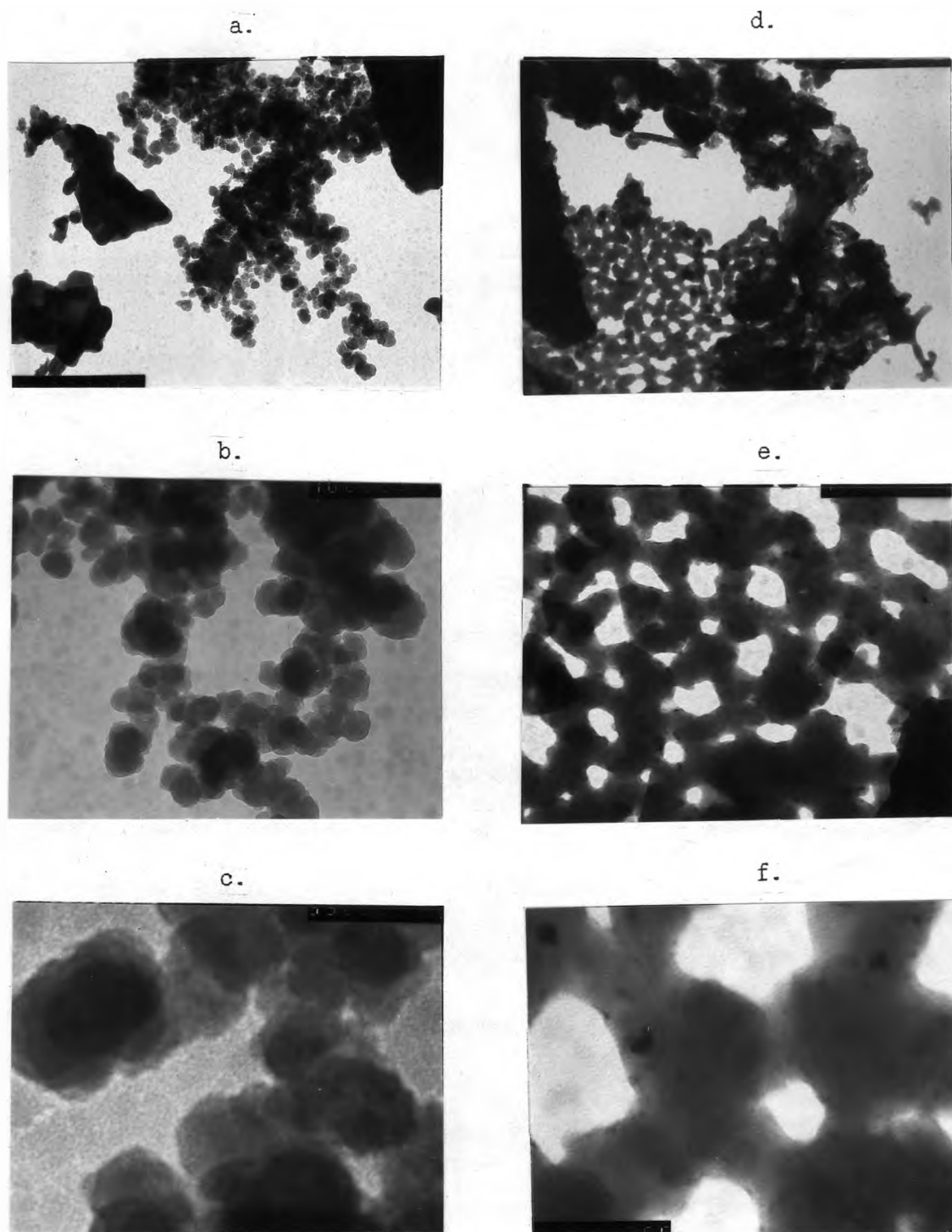
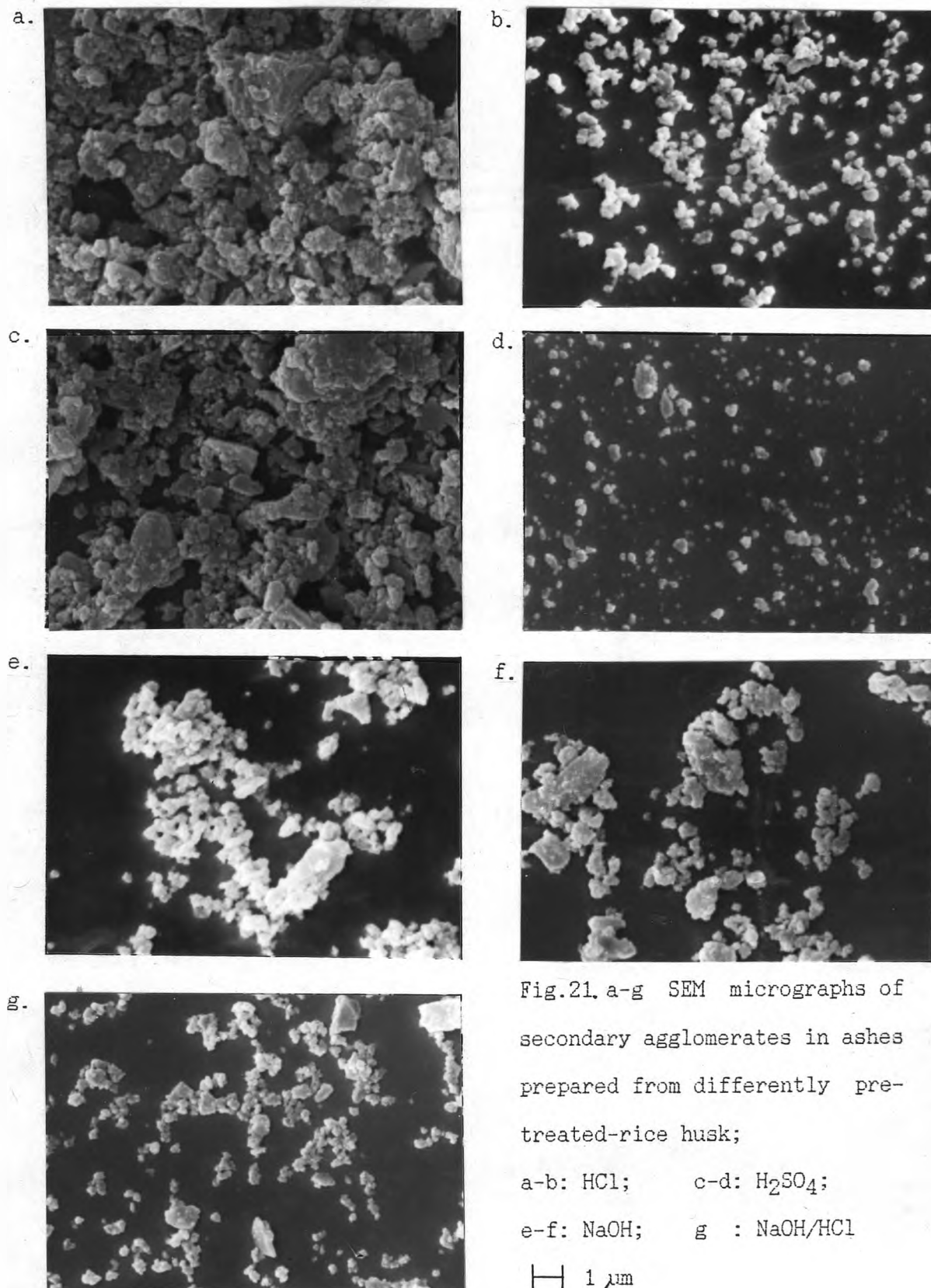


Fig. 20. TEM micrographs from rice husk ash, No pre-treatment (a-c), and NaOH pre-treatment (d-f);

—| a, d: 330 nm; b, e: 100 nm; c, f: 30 nm



As shown on SEM micrographs, rice husk ash has the potential to become a sub-micron size powder.

4.5 Particle Size Distribution and Particle Size Estimation

When the particle size distribution of an amorphous silica is communicated, it is important to clearly refer to a specific level of agglomeration. It is generally accepted to refer to these levels as primary particles (the ultimate level of agglomeration of $[\text{SiO}_4]$ units, typically sized < 1 to a few nm); secondary particles (usually high-coordinate agglomerates of primaries; size depends on pH and solubility and may vary from 5 to 100 nm); higher agglomerates, i.e., agglomerates formed by the secondaries, etc. For a given material, not all levels of agglomeration are necessarily found.

4.5.1 Particle size distribution on TEM and SEM micrographs

The particle size of secondary particles was measured on untreated husk ash first to characterize the particle size distribution provided by nature. The evaluation of TEM micrographs considered at least 300 individual particles. The result is shown in figure 22 (next page).

The diameters for 16, 50, and 84 % abundance, d_{16} , d_{50} , and d_{84} , from integral distribution curve are:

$$d_{16} = 18 \text{ nm}$$

$$d_{50} = 26 \text{ nm}$$

$$d_{84} = 37 \text{ nm}$$

As $d_{50}^2 \approx d_{16} \cdot d_{84}$, the distribution of the particles is supposed to be a logarithmic normal distribution (after DIN 66144) which it actually proves to be (see figure 24). The standard deviation, s , of the distribution is

$$s = (1/2) \cdot \ln(d_{84}/d_{16}) \\ = 0.36$$

which is a narrow distribution.

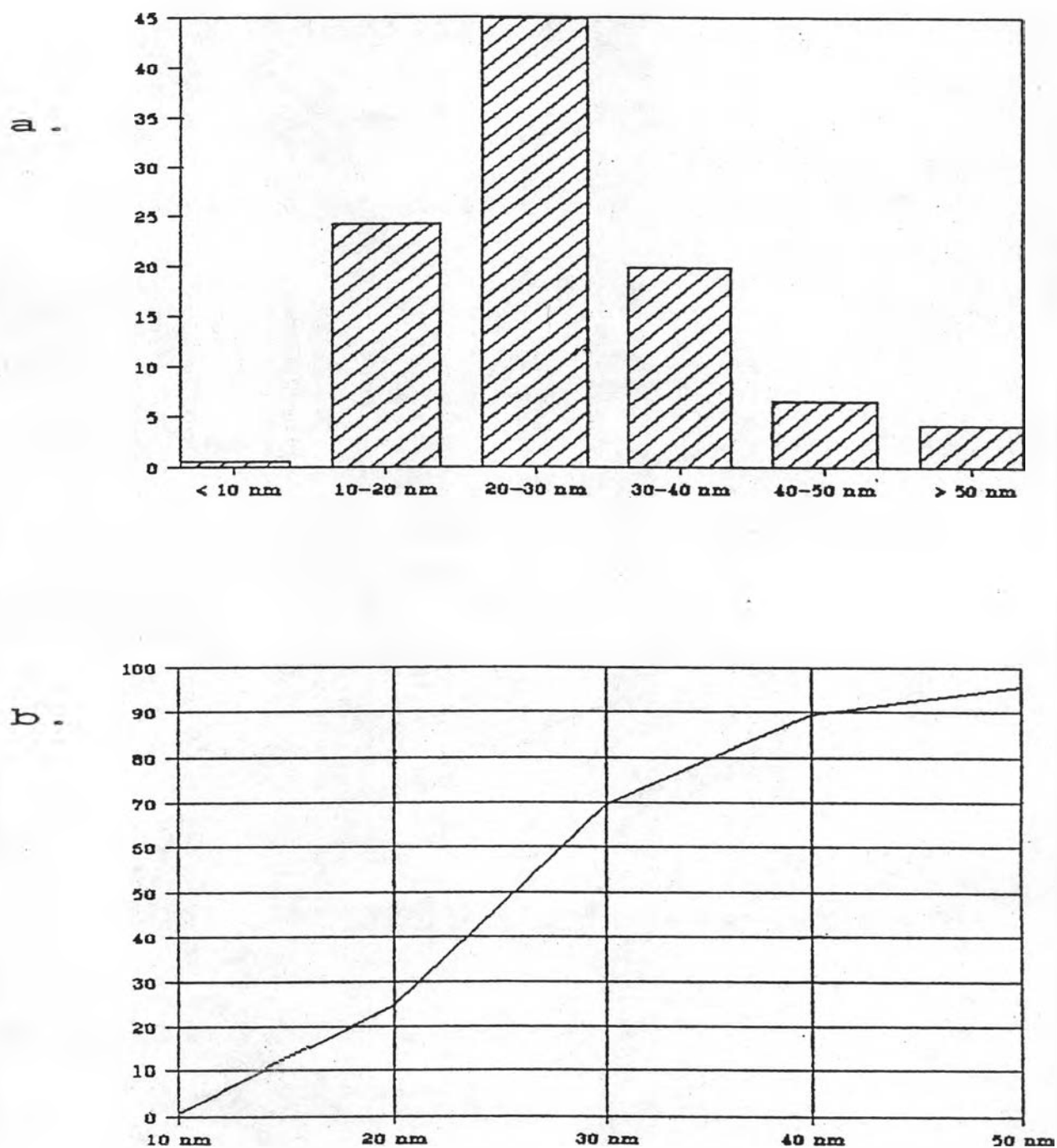


Fig. 22 a-b. Particle size distribution for the secondary particles in silica from untreated husk ash; % abundance
a: differential b: integral

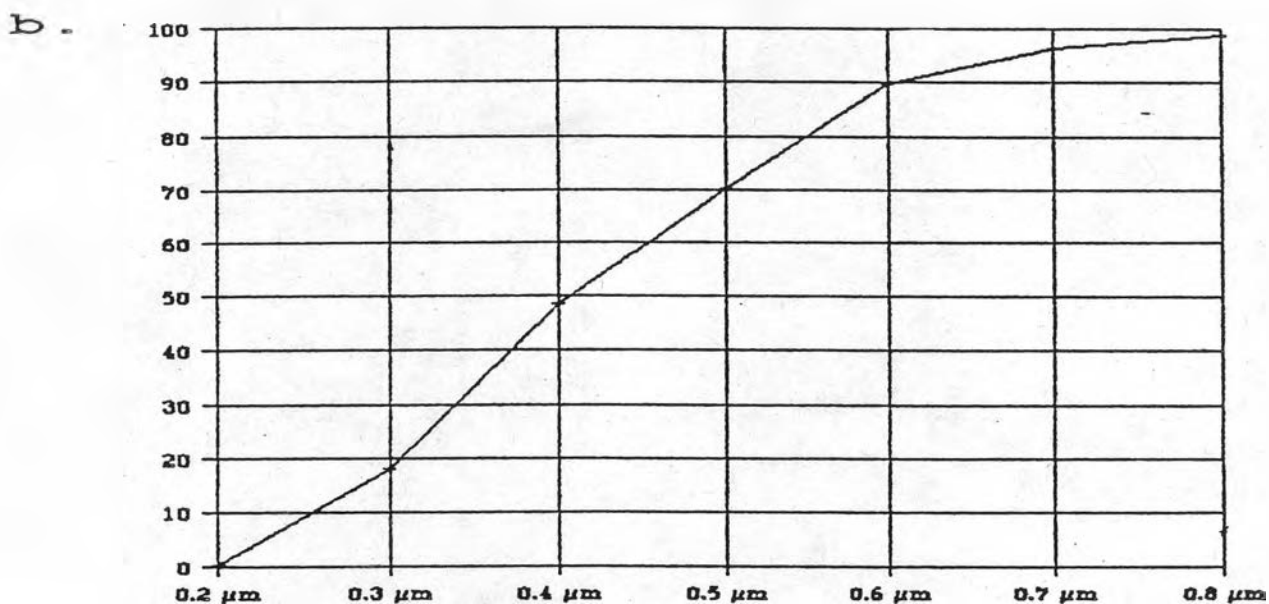
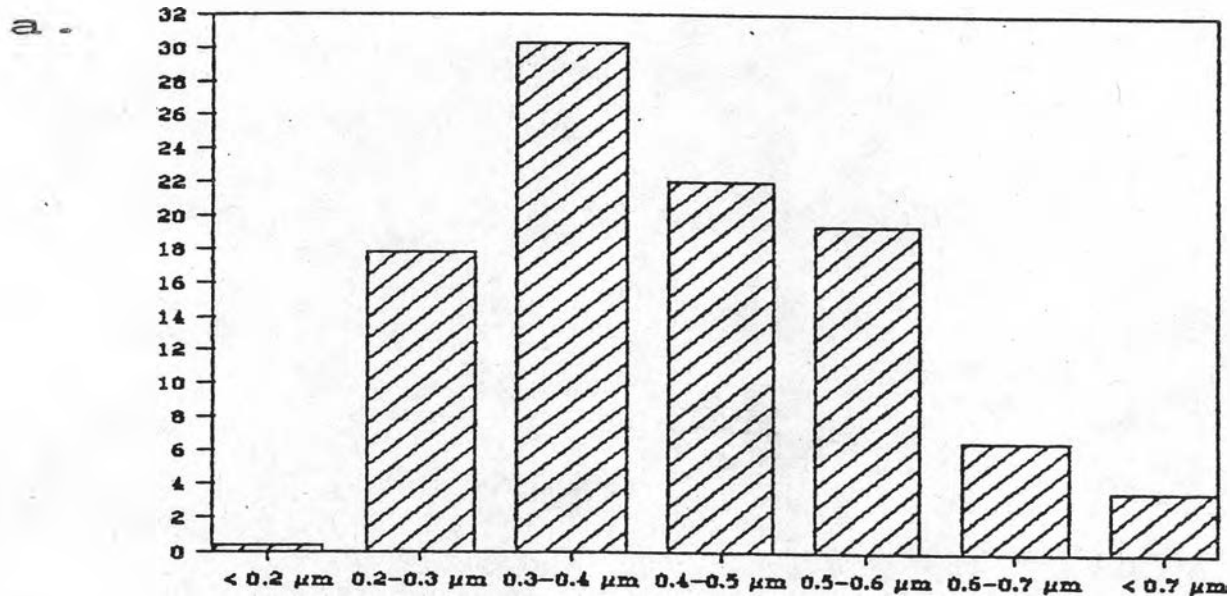


Fig. 23 a-b. Particle size distribution for the tertiary agglomerates in silica from NaOH/HCl pre-treated husk ash; % abundance; a: differential b: integral

For the particle size distribution of tertiary and higher agglomerates, NaOH/HCl treated husk ash was selected, as it was found that the appearance of particles on SEM micrographs depended strongly on sample preparation for SEM. The appearance of agglomerates in the husk ash powder is not correlated to the specific surface area (N_2).

For the evaluation of more than 300 individual particles,

$$d_{16} = 0.3 \mu\text{m}$$

$$d_{50} = 0.4 \mu\text{m}$$

$$d_{84} = 0.6 \mu\text{m}$$

$$\text{and } s = 0.35 \quad (\text{after DIN 66144})$$

which also show very narrow sub-micron sized distribution .

4.5.2 Comparison of particle size distribution from TEM and SEM micrographs to light scattering and sedimentation data.

One of the interesting samples, with high specific surface area and purity, i.e., enzymatic/HCl treated husk ash, was selected to evaluate the size distribution of the still higher levels of agglomeration. The size distribution of these higher order agglomerates followed a power law with $d_{\text{max}} = 31 \mu\text{m}$ and $m = 0.7$; (after DIN 66144)

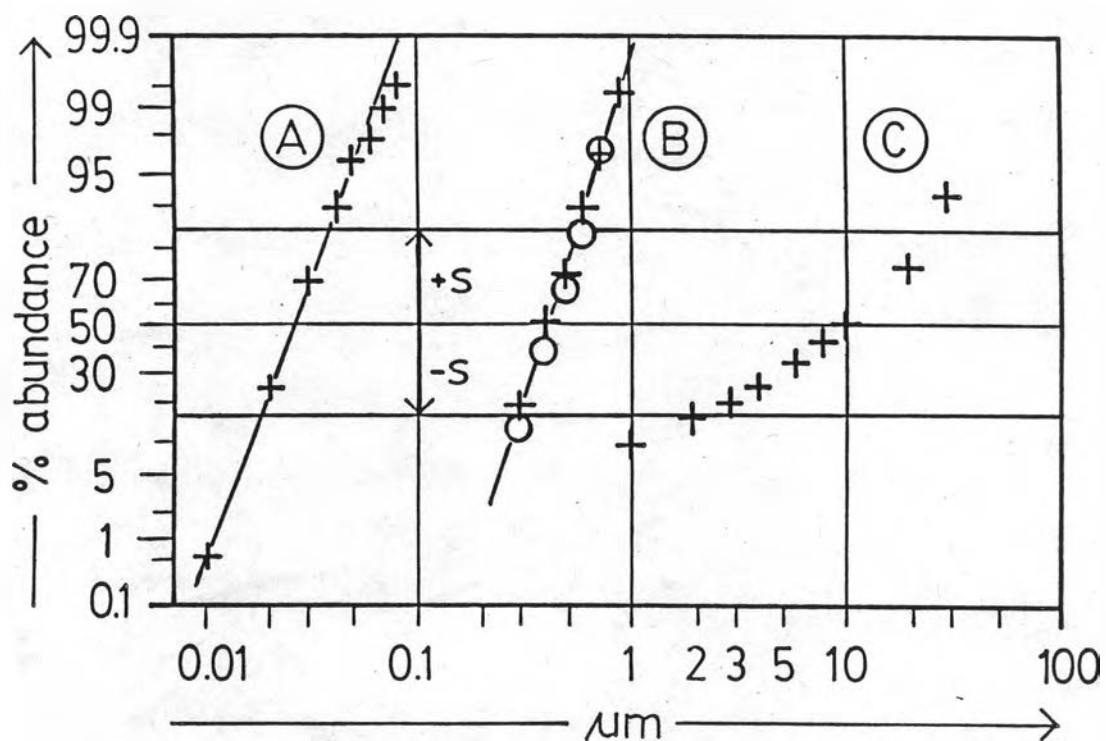


Fig. 24. Particle size distribution of silica particles presented in the log-normal grid after DIN 66144; curve A: secondary particles, No pre-treatment; curve B: tertiary particles, HCl pre-treatment (o), and NaOH/HCl pre-treatment (+); curve C: higher agglomerates, Enzymatic/HCl pre-treatment; straight lines are a guide to the eye.

Specific surfaces can be calculated from the size distributions of powders provided that the considered particles are dense. The specific surface area Γ is given by

$$\Gamma = [6/(\rho \cdot d_{50})] \cdot \exp(s^2/2)$$

for the log-normal distribution and

$$\Gamma = 6m/(\rho d_{\max})$$

for the power law distribution; $\rho = 2.2 \text{ g/cm}^3$. This yields 112, 7.2, and $0.06 \text{ m}^2/\text{g}$ for the secondary particles, tertiary particles, and higher agglomerates, respectively, (see figure 24. A, B, and C curve). The estimate clearly demonstrates that particles larger than the secondaries have little or no influence on the resulting specific surface area.

4.5.3 Particle size estimation

From Scherer's formula, the estimated particle yields d_0 (primary particle size) $\approx 2.4 \text{ nm}$. Table 10 shows the estimation of treated husk ash.

Tab. 10. Particle size estimation from XRD line broadening

treatment	d_0 in nm
None	2.4
HCl	2.4
H ₂ SO ₄	2.3
NaOH	2.7
NaOH/HCl	2.7
HNO ₃	2.5
Enzymatic	2.5
Enzymatic/HCl	2.5
Enzymatic/H ₂ SO ₄	2.3

An estimate of the specific surface area based on the primary particles yields $\Gamma > 1000 \text{ m}^2/\text{g}$. The finding that the specific surface area actually found is 200 to 250 m^2/g (i.e., neither the value of the primaries nor of the secondaries), needs to be discussed.

4.6 Chemical Analysis

Ash samples were analysed for the amount of silica and potassium ion. The results are summarized in table 11.

Tab. 11. Analytical results on rice husk ash

treatment	silica in wt. %	K ₂ O (ppm)
None	96.3 ± 0.6	7338
NaOH	68.3 ± 0.2	na
HCl	99.37 ± 0.15	1375
H ₂ SO ₄	98.99 ± 0.07	530
HNO ₃	98.0 ± 0.4	1900
Enzymatic	96.87 ± 0.15	
	96.84 ± 0.04	
Enzymatic/HCl	99.58 ± 0.13	
	99.43 ± 0.11	
Enzymatic/H ₂ SO ₄	99.56 ± 0.06	
	99.36 ± 0.03	

na - not analysed

*¹) see more detail in Appendix B

4.7 Specific Surface Area

The determination of the specific surface area of treated rice husk ash samples was performed with the one-point areameter described in 3.2.2.7. Only total specific surface area (N_2) but no pore size distribution could be determined. A measuring session consists of the following steps:

- volume calibration,
- initial standard acquisition,
- measurements,
- final standard acquisition.

By this procedure, the total time demand is approx. 4 h. From the above measurement, the following conclusions can be drawn: Systematic bias against the standard, i.e., accuracy; stability of the equipment against systematic drift with time. By repeated measurements, the statistical error or precision was determined. Table 12 presents the results for the specific surface area of different modes of treatment. The values are corrected for systematic bias; the bias itself is given in parentheses. For example, (-10) means: The value originally measured was 10 m^2/g too low. In most cases, repeatability (i.e., precision) was better than $\pm 3 m^2/g$.

Tab. 12. Specific surface area (BET) of treated husk ash

treatment	BET surface (m ² /g)	
None	107	(0)
NaOH	60	(0)
HCl	222	(-3)
HCl*)	253	(-15)
HCl**)	158	(-9)
HCl (2 h-incineration)	255	(-15)
HCl (4 h-incineration)	260	(-15)
HCl (8 h-incineration)	247	(+8)
HCl (700°C; 6 h)	212	(+7)
NaOH/HCl	86	(0)
H ₂ SO ₄	217	(-14)
HNO ₃	250	(0)
Enzymatic	223	(-3)
Enzymatic/HCl	231	(-15)
Enzymatic/H ₂ SO ₄	254	(-16)

*) Measured within one week after incineration

**) Wettened ash, then dry at 110°C overnight before measurement